# Model of Soft Soils under Cyclic Loading

Jing Ni[1], Buddhima Indraratna[2], Xue-Yu Geng[3], John Phillip Carter[4], You-Liang Chen[5]

[1]Lecturer, Department of Civil Engineering, University of Shanghai for Science and Technology, 516 Jungong Road, 200093 Shanghai, PR China. E-mail: wendy_1943@163.com

[2]Professor of Civil Engineering, Centre for Geomechanics and Railway Engineering, Faculty of Engineering, University of Wollongong, Wollongong, NSW 2522, Australia (Corresponding author). E-mail: indra@uow.edu.au

[3]Research Fellow, Centre for Geomechanics and Railway Engineering, Faculty of Engineering, University of Wollongong, Wollongong, NSW 2522, Australia. E-mail: xygeng@gmail.com

[4]Emeritus Professor of Civil Engineering, Centre for Geotechnical Science and Engineering, Faculty of Engineering and Built Environment, University of Newcastle, Newcastle NSW 2308. E-mail: john.carter@newcastle.edu.au

[5]Professor of Civil Engineering, University of Shanghai for Science and Technology, 516 Jungong Road, 200093 Shanghai, PR China. E-mail: chenyouliang2001@163.com

**Abstract:** This paper presents a new constitutive model for cyclic loading of soil to predict the behaviour of soft clays under undrained cyclic triaxial loading. It is inspired by the Modified Cam-clay theory, and a new yield surface for elastic unloading is proposed to capture the soil behaviour under cyclic loading. Only two additional parameters which characterize the cyclic behaviour are employed together with the traditional parameters associated with the Modified Cam-clay constitutive model. The details of the relevant soil properties, initial states, and cyclic loading conditions are presented, and a computational procedure for determining the effective stresses and strains are demonstrated. The new model is used to simulate cyclic triaxial tests on kaolin and the model predictions are generally found to be in agreement with the measured excess pore pressures and axial strains. Furthermore, numerous factors which influence the cyclic performance of soft soils can be considered in the new model, such as the cyclic stress ratios, pre-shearing, and cyclic loading frequency. The critical cyclic stress ratio is also predictable using the proposed model in terms of the excess pore pressures and axial strains.

**Author keywords:** Cyclic model; Soft clay; Cyclic stress ratio; Excess pore pressure; Axial strain.

## Introduction

Attributed to relatively high fines fraction and water content, low-lying soft subgrade soils are often characterized by low bearing capacity, high compressibility and low permeability. The performance of such soils under static loading has been modeled by a number of researchers (Roscoe and Burland 1968; Mita et al. 2004; Karstunen et al. 2012). By contrast, the cyclic behavior of soft subgrade soils is more complex. Excess pore pressure and strain continue to develop with increasing number of cycles, thereby decreasing the bearing capacity of the subgrade and often inducing excessive differential settlement. Therefore, the accumulation of excess pore pressure and excessive plastic deformation of the subgrade under significant cyclic loading is always a major concern for highway pavements, railway tracks and airport runways (Yamanouchi et al. 1975; Kutara et al. 1980; Li and Selig 1996; Chai and Miura 2002).

In the past few decades, experimental research has been devoted to the response of soils and pavement materials to traffic-induced cyclic loads. Factors influencing the cyclic performance of soft soils have been investigated: (i) cyclic stress level which determines whether the soil can reach a non-failure equilibrium state or not (Larew and Leonards 1962; Lashine 1971; Sangrey et al. 1978; Ansal and Erken 1989; Zhou and Gong 2001), (ii) loading frequency which is responsible for the rate of excess pore pressure and axial strains (Takahashi et al. 1980; Yasuhara at al. 1983; Procter and Khaffaf 1984; Hyde et al. 1993; Liu and Xiao 2010), (iii) over-consolidation ratio influencing the effective stress paths and the degradation of the undrained secant shear modulus (Sangrey et al. 1969; Brown et al. 1975; Vucetic and Dobry 1988), and (iv) static pre-shearing which decreases the cyclic shear strength but increases the total shear strength (Seed and Chan 1966; Zimmie and Lien 1986; Ishihara et al. 1993; Hyodo et al. 1994).

By using a considerable body of data obtained from the laboratory tests, cyclic models have been developed. However, most models are empirical and sometimes based on unsubstantiated assumptions or hypotheses, either focusing on just one specific parameter or a combination of two or more conveniently selected parameters within practical limitations. The highlights of a few of these models and their shortcomings are summarised in Table 1. Therefore, more general constitutive models (e.g. Ramsamooj and Alwash 1990; Li and Meissner 2002) are desirable to establish in which various cyclic loading conditions can be considered. However, these models are often complex in terms of the required parameters, whereby some of them cannot be determined directly using conventional equipment, which makes the use of these models in practical situations somewhat limited.

A relatively simple model was proposed by Carter et al. (1980, 1982) based on the Modified Cam-clay theory (Roscoe and Burland 1968). In this model only one additional parameter, which characterizes the cyclic behaviour, is needed along with the Modified Cam-clay parameters, and this can be conveniently determined on the basis of the cyclic triaxial loading tests. However, the generation rate of excess pore pressures predicted by this model increases until the soil ultimately fails, in contrast to the opposite effect observed in some of the previously reported tests (Takahashi et al. 1980; Miller et al. 2000; Zhou and Gong 2001; Sakai et al. 2003). Therefore, a new cyclic model extending that of Carter et al. (1980, 1982) is presented in this paper. In this case, only two additional cyclic degradation parameters are needed (beyond the parameters defining Modified Cam Clay) to represent the yield surface function during elastic unloading. Many factors which influence the cyclic performance of soft soils are considered in this model, such as cyclic stress ratio, pre-shearing, and cyclic loading frequency.

## Framework of the new constitutive cyclic model

### *Assumptions*

For normally consolidated soils, permanent excess pore pressures and strains only occur in the first cycle if the Modified Cam-clay model is strictly used to simulate the cyclic performance. This is because the yield surface remains unchanged after the first load cycle. So the subsequent behaviour of the soil is considered elastic and therefore no further permanent excess pore pressures and strains develop. However, when saturated soft clays are unloaded and then reloaded repeatedly, the permanent excess pore pressures and strains often keep increasing during the entire period of cyclic loading. One way of interpreting this real behaviour is to assume

that the position and perhaps the shape of the yield surface have been influenced in some way by elastic unloading. For simplicity, the form of the yield surface is assumed to remain unchanged, but with a reduced size in an isotropic manner by the elastic unloading. Therefore, a parameter $\theta^*$ is introduced to indicate how much the yield surface contracts when the soil is elastically unloaded (Carter et al. 1980, 1982):

$$\frac{\mathrm{d}p_{\mathrm{c}}^{'}}{p_{\mathrm{c}}^{'}} = \theta^* \frac{\mathrm{d}p_{\mathrm{y}}^{'}}{p_{\mathrm{y}}^{'}} \tag{1}$$

where, $p_{\mathrm{c}}^{'}$ is a hardening parameter which can be considered as the pre-consolidation pressure. $p_{\mathrm{y}}^{'}$ is a variable defined as (Roscoe and Burland 1968):

$$p_{\mathrm{y}}^{'} = p^{'} + \left(\frac{q}{M}\right)^2 \frac{1}{p^{'}} \tag{2}$$

In the above, $M$ is the slope of the critical state line in $p^{'}$ - $q$ space, where $p^{'}$ and $q$ are the effective mean stress and deviator stress defined by the major ($\sigma_1^{'}$) and minor ($\sigma_3^{'}$) principal stresses as $p^{'} = \frac{1}{3}\left(\sigma_1^{'} + 2\sigma_3^{'}\right)$ and $q = \sigma_1^{'} - \sigma_3^{'}$.

In the proposed model, the parameter $\theta^*$ in Eq. (1) is assumed to decrease with the increasing number of cycles, *N*, rather than being constant, taking the form of:

$$\theta^* = \frac{1}{\xi_1 N + \xi_2} \tag{3}$$

where, $\xi_1$ and $\xi_2$ are experimental constants. If $\xi_1 = 0$, then Eq. (3) can be simplified to that of Carter et al. (1980, 1982), whereby assuming $\theta = 1/\xi_2$:

$$\frac{\mathrm{d}p_{\mathrm{c}}^{'}}{p_{\mathrm{c}}^{'}} = \theta \frac{\mathrm{d}p_{\mathrm{y}}^{'}}{p_{\mathrm{y}}^{'}} \tag{4}$$

From Eqs. (1) and (3), it can be seen that for identical conditions, parameters $\xi_1$ and $\xi_2$ determine how much the yield surface contracts when the soil is elastically unloaded, and therefore determining how much excess pore pressures and axial strains are generated for each cycle. As the rate of generation of excess pore pressures and axial strains indicate a corresponding dependence on the period of each cycle (Takahashi 1980; Andersen 2009), the parameters $\xi_1$ and $\xi_2$ are indeed related to the frequency of the applied cyclic loading.

### *Effective stresses and strains during cyclic loading*

The calculation of the effective stresses and strains is demonstrated against the stress path for normally and isotropically consolidated soils under cyclic loading, as shown in Fig. 1. The parameter $p_{\mathrm{cl},i}^{'}$ ($i$ =1, 2·····, $n$) is

the yield stress after the loading part of each cycle, $p'_{\mathrm{cu},i}$ ($i$ =1, 2……, $n$) is the yield stress after the unloading part of each cycle, and $p'_{\mathrm{y},i}$ ($i$ =1, 2……, $n$) is the loading parameter after each cycle.

When the stress path of the soil element moves from point $A'$ to point $A$ during the first loading period, excess pore pressure increases and the effective mean stress decreases. $p'_{\mathrm{cl},1}$ is the yield stress corresponding to point $A$ which can be expressed by:

$$p'_{\mathrm{cl},1} = p'_A + \left(q_A / M\right)^2 p'_A \tag{5}$$

In the above, $q_A$ is equal to the cyclic stress $q_{\mathrm{cyc}}$ and the effective mean stress at point $A$ is given by:

$$\frac{p'_A}{p'_{A'}} = \left( \frac{M^2 + \left(q_A / p'_A\right)^2}{M^2 + \left(q_{A'} / p'_{A'}\right)^2} \right)^{\frac{\lambda-\kappa}{\lambda}} \tag{6}$$

where, $\lambda$ and $\kappa$ are the slopes of the normal compression and swelling lines in $\nu$ - ln $p'$ space, respectively, where $\nu = 1+e$ is the specific volume and $e$ is the void ratio.

During the following unloading period, the stress path travels from point $A$ to $A^*$, and the effective mean stress remains constant. $p'_{\mathrm{y},1}$ is the loading parameter corresponding to point $A^*$. The yield stress for the second cycle or the yield stress after unloading can be calculated as:

$$p'_{\mathrm{cu},1} = p'_{\mathrm{cl},1} \left( \frac{p'_{\mathrm{y},1}}{p'_{\mathrm{cl},1}} \right)^{\theta^*} \tag{7}$$

For the first part of the second cycle, the stress path travels from point $A^*$ to point $B'$ and the soil behaves elastically while $q < q_{\mathrm{yielding}}$. The deviator stress $q_{\mathrm{yielding}}$ causing the re-yielding of the soil can now be given by:

$$q_{\mathrm{yielding}} = \sqrt{\left(p'_{\mathrm{cu},1} - p'_{\mathrm{y},1}\right) M^2 p'_{\mathrm{y},1}} \tag{8}$$

Afterwards, the stress path moves from point $B'$ to $B$ ($q_{\mathrm{yielding}} < q < q_{\mathrm{cyc}}$) and the effective mean stress decreases. During this period, the soil behaves plastically.

### *Computational procedure*

The procedure for calculating the excess pore pressures and strains generated under cyclic loading is explained in Fig. 2. The important steps are elaborated as follows.

Essential parameters

The parameters that need to be determined include:

(1) soil properties, viz., the slopes of the normal (virgin) compression line ( $\lambda$ ), swelling line ( $\kappa$ ), and the critical state line in $p'$ - $q$ space ( $M$ ), shear modulus ( $G$ ), and pre-consolidation stress $p'_{c0} = \left(\sigma'_{1c} + 2\sigma'_{3c}\right)/3$, where $\sigma'_{1c}$ and $\sigma'_{3c}$ are the major and minor principal stresses after initial consolidation but prior to unloading or any cyclic loading;

(2) initial soil states, viz., the effective mean stress ( $p'_0$ ), deviator stress ( $q_0$ ), and specific volume ( $v_0 = 1 + e_0$ ) prior to cyclic loading; and

(3) cyclic loading conditions, viz., the cyclic deviator stress ( $q_{cyc}$ ), cyclic loading frequency ( $f$ ), and cyclic degradation parameters ( $\xi_1$ and $\xi_2$ ).

Set up steps and sub-steps

Each loading and unloading step can be further divided into sub-steps, e.g., $q_{cyc}$ can be divided into a number of increments (say $n$ ), then each step has an incremental deviator stress ( $dq_i$ ) ( $i$ =1, 2, 3… $n$ ). Based on the notation of the deviator stress ( $dq_i$ ) ( $i$ =1, 2, 3… $n$ ) and the state of the soil, the process of cyclic loading can be divided into three categories: (1) $dq_i < 0$, soil is unloaded and behaves elastically; (2) $dq_i > 0$ and $p'_y < p'_c$, soil is reloaded and behaves elastically; (3) $dq_i > 0$ and $p'_y = p'_c$, soil is reloaded and behaves in a plastic manner. Then the corresponding processes as mentioned in the previous section can be applied to calculate the excess pore pressures and strains.

## Cyclic triaxial loading tests on kaolinite

A series of undrained cyclic triaxial loading tests was conducted on specimens of reconstituted kaolinite, 38 mm in diameter by 76 mm high. The soil had the following properties: specific gravity $G_s = 2.7$, liquid limit $w_L = 55\%$, plastic limit $w_p = 27\%$, compression index $C_c = 0.42$ ($\lambda \approx 0.182$), and swelling index $C_s = 0.06$ ($\approx 0.026$). Each of the specimens was subjected to an initial effective vertical stress of 40 kPa to represent the in situ stress and consolidated in the triaxial cell under anisotropic conditions ( $k_0 = 0.6$ ).

The undrained cyclic loading tests were carried out using a triaxial loading apparatus which comprised the axial loading unit (dynamic actuator), an air pressure and water control unit, a pore pressure measurement system and a volumetric change measurement device. Excess pore pressure was measured through the drainage valve at the base of the specimen. Conventional monotonic triaxial tests were conducted to obtain the maximum deviator stress at failure ( $s_{u0}$ ) during static loading. Then the cyclic stress ratio was defined as the ratio of cyclic stress to the maximum deviator stress at failure ( $CSR = q_{cyc} / s_{u0}$ ). All the test conditions are given in Table 2.

## Verification of the new cyclic model

The parameters for the new constitutive model including soil properties, initial states, and cyclic loading conditions are provided in Tables 3 and 4. The values of cyclic degradation parameters $\xi_1$ and $\xi_2$ given in Table 4 indicate that the effect of cyclic stress ratio on the cyclic degradation parameters is negligible.

Furthermore, $\xi_2$ increases with the increasing loading frequency, which implies that less excess pore pressure may be generated at a higher loading frequency. Takahashi (1980) proposed that the rate of generation of excess pore pressure would indicate a corresponding dependence on the loading frequency, e.g., for identical cycles, higher excess pore pressure is generated at a lower loading frequency. This observation is consistent with the study by Andersen (2009), where more cycles were needed to bring the specimen to failure at a higher frequency. However, in the proposed model the loading frequency is not an input parameter and the model has no intrinsic rate component, so therefore there needs to be an alternative input to represent the effect of the loading frequency. As indicated by the experimental results, $\xi_2$ depends on the loading frequency (Fig. 3), where the corresponding plot of $\xi_2$ versus $\log f$ is expressed as a linear relationship.

The simulation together with the test data of normalized excess pore pressures and axial strains against the number of cycles for specimens tested under 0.1 Hz and 5 Hz is shown in Fig. 4. Acceptable agreement is found between the predicted results and the actual trends. As expected, both normalized excess pore pressures and axial strains increase with the increasing cyclic stress ratio. The plots shown in Fig. 4 clearly suggest that the excess pore pressure rises quickly at the initial stages, and continues to increase gradually with the number of cycles. For stable specimens ( CSR = 0.4 and 0.6), the excess pore pressures reach a stable state after their initial rapid development, with the final normalized excess pore pressures equaling 0.2 and 0.4 for $\mathrm{CSR} = 0.4$ and 0.6, respectively. For failed specimens, the excess pore pressures develop so quickly that the critical normalized value of 0.6 is reached in the first few cycles. Failure of the specimen occurs before a stable state can be reached. It should be noted that there is no failure indicated for any of the samples by simply looking at these normalized excess pore pressures alone. In contrast, the failure of the two samples $\mathrm{U}_{03}$ and $\mathrm{U}_{12}$ ( CSR = 0.8) is characterized by a dramatic rise in axial strains beyond a critical number of cycles. While the failure of $\mathrm{U}_{03}$ ( $f$ = 0.1 Hz) occurs as $N$ approaches 2,000, for the highest frequency, i.e., $\mathrm{U}_{12}$ at $f$ = 5 Hz, the failure occurs as $N$ > 30,000 cycles. For specimens with $\mathrm{CSR} = 0.4$ and 0.6, the axial strains are quite small (less than 1%) at the end of the tests. It is indicated that a rapid upward trajectory of the axial strains occurs when a normalized excess pore pressure of 0.6 is reached, as reflected by the comparison of excess pore pressures and axial strains for the specimens tested under $\mathrm{CSR} = 0.8$.

## Undrained Cyclic Model Analysis

In this section, the effects of cyclic stress ratio, anisotropic consolidation condition and cyclic degradation parameters $\xi_1$ and $\xi_2$ on the development of excess pore pressure and axial strains are investigated using the proposed cyclic model. The basic soil properties assumed in this parametric study are given in Table 5.

### *Effect of cyclic stress ratio*

To investigate how the cyclic stress level affects the performance of soft soils, the predictions of normalised excess pore pressures and axial strains at various cyclic stress ratios using the proposed model are shown in Fig. 5. The results plotted in Fig. 5(a) indicate that the critical cyclic stress ratio is around 0.5 (shown by the dashed

line), for the parameters used. When CSR = 0.6, 0.7, and 0.8, the excess pore pressure increases very fast such that the value of $u_f / p'_{c0}$ (where $u_f$ represents the excess pore pressure at failure) reaches 0.8 in the first few cycles. When CSR = 0.2, 0.3, and 0.4, the rates of excess pore pressure generation decrease and the specimens reach a stable state after an initial stage of rapid development. The determination of the critical cyclic stress ratio is made easier by observing the axial strains, as shown in Fig. 5 (b). At a critical cyclic ratio of 0.5, the axial strain at 1,000 cycles is around 7%, which is seven times that at CSR = 0.4, compared to twice for the excess pore pressures.

When $\xi_2$ increases from 10 to 50, the predictions of normalised excess pore pressures and axial strains are shown in Fig. 6. These results indicate that the cyclic stress ratio becomes critical at around 0.6. Comparison of Figs. 5 and 6 suggest that an increased critical cyclic stress ratio from 0.5 to 0.6 is determined when $\xi_2$ increases from 10 to 50.

### *Effect of anisotropic consolidation ratio*

To investigate how the initial anisotropic consolidation stress ratio ( $k_0 = \sigma'_{3c} / \sigma'_{1c}$ ) influences the performance of this soft soil, the predictions made by the proposed model under various anisotropic consolidation conditions are given in Figs. 7 and 8. As shown in Fig. 7, five consolidation stress ratios from 0.6 to 1.0 with 0.1 intervals are considered and in each case $\xi_1 = 1$ and $\xi_2 = 100$. For a relatively low cyclic stress ratio CSR = 0.3, the soft soil behaves in a stable manner under cyclic loading when $k_0$ = 0.8, 0.9, and 1.0. When $k_0$ decreases to 0.7, even at CSR = 0.3, the excess pore pressure and axial strain build up significantly, and failure occurs around 400 cycles. With an even smaller anisotropic consolidation stress ratio at $k_0$ = 0.6, the excess pore pressure and axial strain increase so rapidly that the soil would fail within fewer cycles, around 100 cycles. For a medium cyclic stress ratio CSR = 0.5, the effect of different anisotropic consolidation conditions is presented in Fig. 8. These predictions indicate that only the isotropically consolidated soil ( $k_0$ = 1.0) is stable when subjected to cyclic loading. For instance, when $k_0$ decreases to 0.9, excess pore pressure and axial strain accumulate to a significant magnitude, and failure occurs around 980 cycles. With a decreasing value of $k_0$ from 0.8 to 0.6, the number of cycles at failure decreases from 200 to just 5 cycles. The comparison of Figs. 7 and 8 indicates that while the minimum value of $k_0$ is 0.8 at CSR = 0.3 to sustain cyclic stability, it increases to unity at CSR = 0.5.

In summary, the model predicts that the anisotropic consolidation stress ratio has an effect on the behaviour of soft clays subjected to cyclic loading. For a given cyclic stress ratio, the excess pore pressure and axial strain increase as the consolidation stress ratio increases. A stable state can be reached at a relatively large value of $k_0$, while failure could occur at a small value of $k_0$. The number of cycles at failure decreases with a decreasing value of $k_0$. When the cyclic stress ratio increases, an increased value of $k_0$ should be applied during the process of consolidation to ensure that the soft clay behaves in a stable manner.

The effect of the anisotropic consolidation stress ratio on the critical cyclic stress ratio is shown in Figs. 9 and 10. For $k_0$ = 0.82, the development of excess pore pressure and axial strain is shown in Fig. 9. The

predictions indicate that the critical cyclic stress ratio is about 0.4. When the cyclic stress ratio is above this critical level, the excess pore pressure develops rapidly and the value of $u_f / p'_{c0}$ increases to 0.81. When the cyclic stress ratio is below the critical value, the excess pore pressure develops in a more gradual or stable manner after the initial stage of cycling. The axial strain at $CSR > 0.4$ continues to rise at an increasing rate, which causes failure of the specimen soon after the cyclic loading commences. For $CSR < 0.4$, the rate of axial strain development is relatively small (i.e., less than 1%) at 1,000 cycles.

For a decreased consolidation stress ratio $k_0$ = 0.68, the generation of excess pore pressure and axial strain is shown in Fig. 10. Here, a smaller critical cyclic stress ratio of 0.3 is observed compared to that under $k_0$ = 0.82. The comparison of Figs. 9 and 10 indicates that a reduced value of $u_f / p'_{c0}$ from 0.81 to 0.78 is observed when the consolidation stress ratio decreases from 0.82 to 0.68. When $CSR > 0.3$, the excess pore pressure and axial strain increase significantly and the failure is shown to occur at around 150 cycles with an asymptotic increase in axial strain. When the cyclic stress ratio is below the critical value $CSR < 0.3$, the excess pore pressure and axial strain develop in a stable manner.

In summary, the value of critical cyclic stress ratio is influenced by the anisotropic consolidation stress ratio. Usually the critical cyclic stress ratio decreases with a decreasing value of consolidation stress ratio. Furthermore, the value of $u_f / p'_{c0}$ decreases with a decreasing value of $k_0$. It is implied that to ensure the stability of a soft clay subgrade, a cyclic load with a smaller $q_{cyc}$ is preferred when the soil is preconsolidated under a smaller ratio of $\sigma'_{3c} / \sigma'_{1c}$. This analysis also confirms the conclusion by some other researchers (e.g., Zimmie and Lien 1986; Andersen 1988; Ishihara et al. 1993) that the lower the value of $k_0$, the less the cyclic resistance of soft soil to cyclic loading.

### *Effect of cyclic degradation parameters*

The influence of cyclic degradation parameter $\xi_1$ on the development of excess pore pressures and axial strains is shown in Fig. 11. The predicted results indicate that the rate of generation of excess pore pressures and axial strains decreases as the value of $\xi_1$ increases. When $\xi_1$ changes from 0 to 5, the number of cycles to failure also increases. Failure does not occur at higher values of $\xi_1$. To investigate the influence of the cyclic degradation parameter $\xi_2$, two particular cases will be discussed: (a) $\xi_1 = 0$ which represents the special situation that coincides with the cyclic model of Carter et al. (1980, 1982); and (b) $\xi_1 \neq 0$.

The development of excess pore pressure and axial strain versus the number of loading cycles for $\xi_1 = 0$ is shown in Fig. 12, where the value of $\xi_2$ ranges from 50 to 300 at intervals of 50. As expected, the predicted results indicate that the rate and magnitude of excess pore pressure and axial strain decrease as the value of $\xi_2$ increases. The results plotted in Fig. 12(a) also indicate that the rate of generation of excess pore pressure increases with the increasing number of loading cycles, regardless of the value of $\xi_2$.

When $\xi_1 = 0$, the effect of the level of cyclic stress on the development of excess pore pressures and axial strains is shown in Fig. 13. The data shown in Fig. 13(a) indicate that the rate of increase of excess pore pressures does not decrease with an increasing number of loading cycles for a cyclic stress ratio ranging from 0.2 to 0.8, in contrast to the opposite effect observed in some of the previously reported tests (Takahashi et al. 1980; Miller et al. 2000; Zhou and Gong 2001; Sakai et al. 2003), where a decreased rate of excess pore pressure is anticipated, especially for a low cyclic stress ratio. Unfortunately, for $\xi_1 = 0$, the critical cyclic stress ratio could not be distinctly identified because of similar trends of all excess pore pressure plots regardless of the value of the cyclic stress ratio. In the same way, the critical cyclic stress ratio could not be predicted from the axial strains plots either as shown in Fig. 13(b). Nevertheless, the number of cycles to cause failure rapidly decreases when CSR increases from 0.2 to 0.8.

The relationships between $1/\xi_2$ and the number of cycles at failure ( $N_f$ ) for different cyclic stress ratios are plotted in Fig. 14. The effect of $\xi_1$ on the number of cycles at failure is also considered in the way that predictions are made for $\xi_1$= 0, 0.1 and 0.5, respectively. It is clear that at a constant cyclic stress ratio, the number of cycles to cause failure decreases as the value of $1/\xi_2$ increases. In addition, at a constant value of $1/\xi_2$, the number of cycles to failure decreases as the cyclic stress ratio increases. For identical parameters, the number of cycles at failure increases as $\xi_1$ increases. The cyclically generated excess pore pressures and axial strains for $\xi_1 \neq 0$ are shown in Fig. 15, with the values of $\xi_2$ changing from 50 to 300 in increments of 50. The results indicate that the generation of excess pore pressures and axial strains decreases as the value of $\xi_2$ increases.

In essence, the excess pore pressure and axial strains decrease as the cyclic degradation parameters $\xi_1$ and $\xi_2$ increase in magnitude. For $\xi_1 = 0$ (Carter et al. 1980, 1982), the critical cyclic stress ratio is not predictable by simply detecting the development of excess pore pressure and axial strains, whereas when $\xi_1 \neq 0$ (i.e., the proposed model), a dramatic increase in both excess pore pressure and axial strain is observed when the cyclic stress ratio increases towards a critical value.

### Limitations of the Current Study

Within the scope of this study, the authors were able to test experimentally only one type of soft clay, and the results of these laboratory tests were used to validate the proposed cyclic soil model as well as to conduct a parametric analysis in order to understand and characterize the cyclic behaviour with the aid of two cyclic degradation parameters ( $\xi_1$ and $\xi_2$ ). In order to instill greater confidence in the use of the model and these two parameters, further testing on other types of clay soils over a broader range of frequencies is highly desirable. This will enable better understanding and quantification of the role of the initial state of the soil and the nature of cyclic loading, including the possible dependence of these two parameters on the loading frequency. In other words, the values of the cyclic degradation parameters specific to this study should not be readily adopted to

other soil types or when subjected to different cyclic loading conditions. In order to predict the cyclic soil behaviour accurately, the values of the degradation parameters need to be evaluated on a case by case basis.

## Conclusions

A new cyclic model to simulate the behaviour of soft soils under repeated loading is proposed in this paper extending that of Carter et al. (1980, 1982). In the proposed model, only two additional cyclic degradation parameters ($\xi_1$ and $\xi_2$) are needed together with the traditional modified Cam-clay parameters. The values of these two cyclic degradation parameters can be determined from undrained cyclic triaxial tests. The development of excess pore pressures and axial strains against the number of loading cycles for various cyclic loading conditions was studied, and the following conclusions could be drawn:

1. Good agreement is found between the predicted results of excess pore pressure and axial strain from a series of undrained cyclic triaxial loading tests conducted on specimens of kaolinite. Cyclic degradation parameter $\xi_1$ is a soil property which is independent of the loading frequency, while $\xi_2$ increases with the magnitude of loading frequency. Furthermore, the effect of cyclic stress ratio on the cyclic degradation parameter is negligible.
2. For $\xi_1 = 0$ which is a special case of the proposed cyclic model that captures the original model of Carter et al. (1980, 1982), the critical stress ratio is not predictable by solely detecting the development of excess pore pressure and axial strain. In contrast, for the current model with $\xi_1 \neq 0$, a dramatic increase in both excess pore pressure and axial strain is observed when the cyclic stress ratio increases to a critical value.
3. The excess pore pressures and axial strains decrease with the increasing values of the cyclic degradation parameters $\xi_1$ and $\xi_2$. Therefore, the number of loading cycles at failure also increases when $\xi_1$ and $\xi_2$ increase.
4. The influence of cyclic stress ratio on the excess pore pressure and axial strain was studied, and it was found that with the increasing magnitude of cyclic stress ratio, the number of loading cycles to initiate failure would decrease.
5. The initial shear stress has a significant effect on the cyclic performance of the clay specimen. With the initial shear stress, the critical cyclic stress ratio seems to decrease compared to specimens with no pre-shearing. In addition, the excess pore pressure at failure is reduced due to the initial shear stress.

## Acknowledgments

The authors acknowledge the support of Innovative Research Project of Shanghai Municipal Education Commission (Project number 14YZ081), Young Teacher Training Scheme of Shanghai Municipal Education Commission (Project number slg13027), and the Australian Research Council (ARC) for funding of this research.

## Notation

*The following symbols are used in this paper:*

CSR = cyclic stress ratio CSR = $q_{cyc} / s_{u0}$

$D^e$, $D^p$ = matrix for incremental stress-strain law when a stress state is elastic and plastic, respectively

$e$ = void ratio

$f$ = cyclic loading frequency

$G$ = shear modulus

$G_s$ = specific gravity

$M$ = slope of the critical state line in $p'$ - $q$ space

$N$ = number of loading cycles

$p'$ = effective mean stress

$p'_c$ = hardening parameter which can be considered as pre-consolidation pressure

$p'_{cl,i}$ = yield stress after the loading part of each cycle

$p'_{cu,i}$ = yield stress after the unloading part of each cycle

$p'_y$, $p'_{y,i}$ = loading parameter

$q$ = deviator stress

$q_{cyc}$ = cyclic deviator stress

$s_{u0}$ = maximum deviator stress at failure for static loading

$q_{yielding}$ = deviator stress causing the re-yielding of the soil for each cycle

$u$ = excess pore pressure

$\nu$ = specific volume

$\varepsilon_s$, $\varepsilon_s^e$, $\varepsilon_s^p$ = shear, elastic shear, and plastic shear stresses

$\varepsilon_v$, $\varepsilon_v^e$, $\varepsilon_v^p$ = volumetric, elastic volumetric, and plastic volumetric stresses

$\kappa$ = slope of the swelling line in $\nu$ - $\ln p'$ space

$\lambda$ = slope of the normal compression line in $\nu$ - $\ln p'$ space

$\theta$ = $\theta = 1/\xi_2$

$\theta^*$ = $\theta^* = \dfrac{1}{\xi_1 N + \xi_2}$

$\sigma'_1$, $\sigma'_{1c}$ = major principal stresses

$\sigma'_3$, $\sigma'_{3c}$ = minor principal stresses

$\xi_1$, $\xi_2$ = cyclic degradation parameters

## References


Andersen, K. H. (2009). "Bearing capacity under cyclic loading – offshore, along the coast, and on land. The 21th Bjerrum Lecture presented in Oslo, 23 November 2007." *Can. Geotech. J.*, 46(5), 513–535.

Ansal, A. M., and Erken, A. (1989). "Undrained behavior of clay under cyclic shear stresses." *J. Geotech. Eng.*, 115(7), 968–983.

Brown, S. F., Lashine, A. K. F., and Hyde, A. F. L. (1975). "Repeated load triaxial testing of a silty clay." *Geotechnique*, 25(1), 95–114.

Chai, J. C., and Miura, N. (2002). "Traffic-load-induced permanent deformation of road on soft subsoil." *J. Geotech. Geoenviron. Eng.*, 128(11), 907–916.

Carter, J. P., Booker, J. R., and Wroth, C. P. (1980). "The Application of a Critical State Soil Model to Cyclic Triaxial Tests." *Proc., 3rd Australia-New Zealand Conf. Geomech.*, Wellington, N.Z., 2, 121–126.

Carter, J. P., Booker, J. R., and Wroth, C. P. (1982). "A critical state soil model for cyclic loading." Soil mechanics-transient and cyclic loading, Chichester: John Wiley & Sons, 219–252.

Hyde, A. F. L., Yasuhara, K., and Hirao, K. (1993). "Stability caritеria for marine clay under one-way cyclic loading." *J. Geotech. Engrg.*, 119(11), 1771–1789.

Hyodo, M., Yamamoto, Y., and Sugiyama, M. (1994). "Undrained cyclic shear behaviour of normally consolidated clay subjected to initial static shear stress." *Soils Found.*, 34(4), 1–11.

Ishihara, K. (1993). “Dynamic Properties of Soils and Gravels from Laboratory Tests.” *Soil Dynamics and Geotechnical Engineering*, Seco e Pinto ed., Balkema, Rotterdam, 1–17.
Karstunen, M., Rezania, M., Sivasithamparam, N., and Yin, Z. (2012). “Comparison of Anisotropic Rate-Dependent Models for Modelling Consolidation of Soft Clays.” *Int. J. Geomech.*, 10.1061/(ASCE)GM.1943-5622.0000267 (Nov. 3, 2012).
Kutara, K., Miki, H., Mashita, Y., and Seki, K. (1980). ‘‘Settlement andcountermeasures of the road with low embankment on soft ground.’’ *Tech. Rep. of Civil Eng.*, 22(8), 13–16 (in Japanese).
Larew, H. G., and Leonards, G. A. (1962). “A strength criterion for repeated loads.” *Highway Research Board Proceedings*, 41, 529–556.
Lashine, A. K. (1971). “Some aspects of the characteristics of Keuper marl under repeated loading.” Ph.D. thesis, University of Nottingham, Nottingham, U. K.
Li, T., and Meissner, H. (2002). “Two-surface plasticity model for cyclic undrained behavior of clays.” *J. Geotech. Geoenviron. Eng.*, 128(7), 613–626.
Li, D. Q., and Selig, E. T. (1996). “Cumulative plastic deformation for fine grained subgrade soils.” *J. Geotech. Engrg.*, 122(12), 1006–1013.
Liu, J. K., and Xiao, J. H. (2010). “Experimental study on the stability of railroad silt subgrade with increasing train speed.” *J. Geotech. Geoenviron. Eng.*, 136(6), 833–841.
Mita, K., Dasari, G., and Lo, K. (2004). ”Performance of a Three-Dimensional Hvorslev–Modified Cam Clay Model for Overconsolidated Clay.” *Int. J. Geomech.*, 4(4), 296–309.
Miller, G. A., Ten, S. Y., and Li, D. (2000). “Cyclic shear strength of soft railroad subgrade.” *J. Geotech. Geoenviron. Eng.*, 126(2), 139–147.
Procter, D. C., and Khaffaf, J. H. (1984). “Cyclic triaxial tests on remoulded clays.” *J. Geotech. Engrg.*, 110(10), 1431–1445.
Ramsamooj, D. V., and Alwash, A. J. (1990). “Model prediction of cyclic response of soils.” *J. Geotech. Engrg.*, 116(7), 1053–1072.
Roscoe, K. H., and Burland, J. B. (1968). “On the generalized stress–strain hehaviour of ‘wet’ clay.” Engineering Plasticity, Cam-bridge University Press, 535–609.
Sakai, A., Samang, L., and Miura, N. (2003). “Partially-drained cyclic hehavior and its application to the settlement of a low embankment road on silty-clay.” *Soil Found.*, 43(1), 33–46.
Sangrey, D. A., Henkel, D. J., and Esrig, M. I. (1969). “The effective stress response of a saturated clay soil to repeated loading.” *Can. Geotech. J.*, 6, 241–252.
Sangrey, D. A., Polard, W. S., and Egan, J. A. (1978). “Errors associated with rate of undrained cyclic testing of clay soils. In Cyclic geotechnical testing.” ASCE, Special Technical Publication STP 654, 280–294.
Seed, H. B., and Chan, C. K. (1966). “Clay Strength under Earthquake Loading Conditions.” *Proc. Amer. Soc. Civil Eng.* vol. 92, SM2, pp. 53–78.
Takahashi, M., Hight, D. W., and Vaughan, P. R. (1980). “Effective stress changes observed during undrained cyclic triaxial tests on clay.” *International Symposium on Soils under Cyclic and Transient Loading*, Swansea, 7-11 January, 201–209.
Vucetic, M., and Dobry, R. (1988). “Degradation of marine clays under cyclic loading.” *J. Geotech. Engrg.*, 114(2), 133–149.
Yamanouchi, T., and Yasuhara, K. (1975). “Settelement of clay subgrade after opening to traffic.” *Proc., 2nd Australia and New Zealand Conf. Geomech.*, Vol.1, Brisbane, pp.115–200.
Yasuhara, K., Ue, S., and Fujiwara, H. (1983). “Undrained shear behaviour of quasi-overconsolidated clay.” *Proc. IUTAM Symp. On Seabed Mech.*, Graham and Trotman, London, England, 17–24.
Zhou, J., and Gong, X. N. (2001). “Strain degradation of saturated clay under cyclic loading.” *Can. Geotech. J.*, 38, 208–212.
Zimmie, T. F., and Lien, C. Y. (1986). “Response of clay subjected to combined cyclic and initial static shear stress.” Proc. *3rd Can. Conf. on Marine Geotech. Engrg.*, [S.l.]: [s.n.], 655–675.

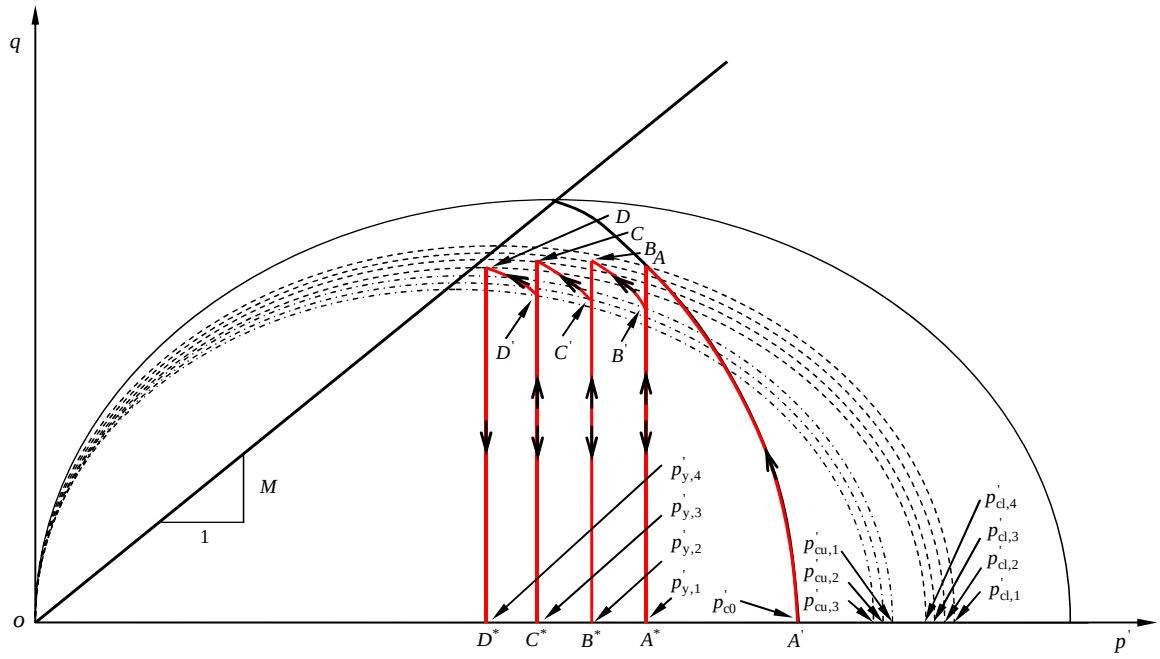


**Fig. 1.** The stress path for cyclic loading

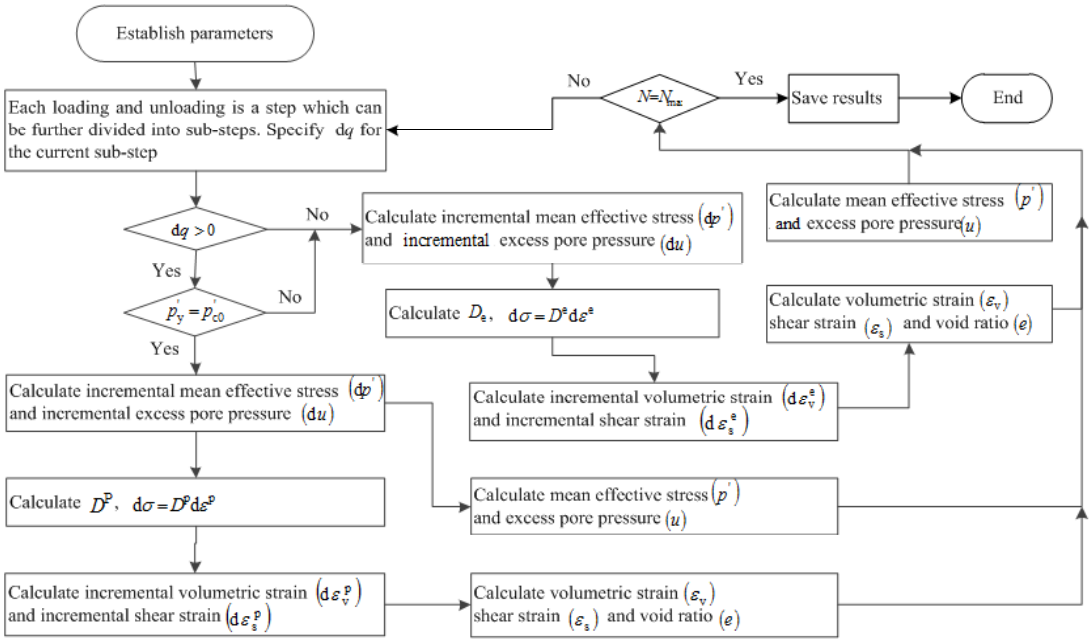


**Fig. 2.** Computational Procedure

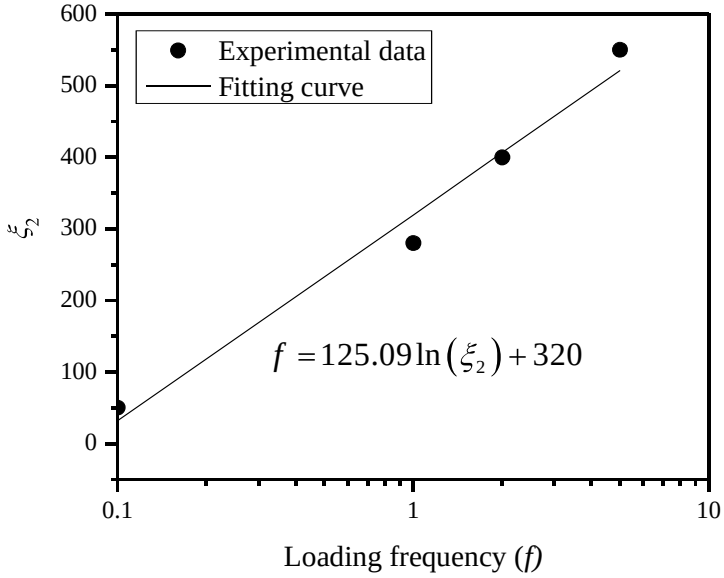


**Fig. 3.** The relationship between $\xi_2$ and loading frequency $f$

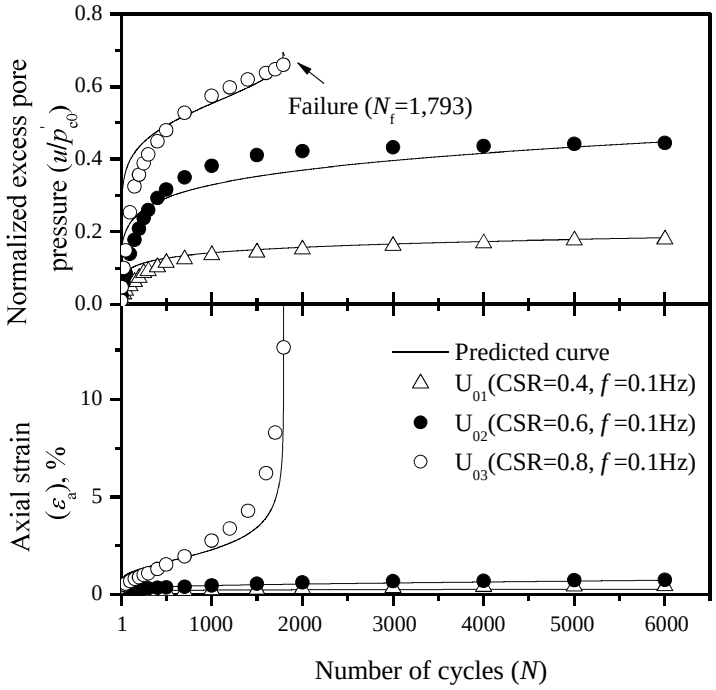


(a)

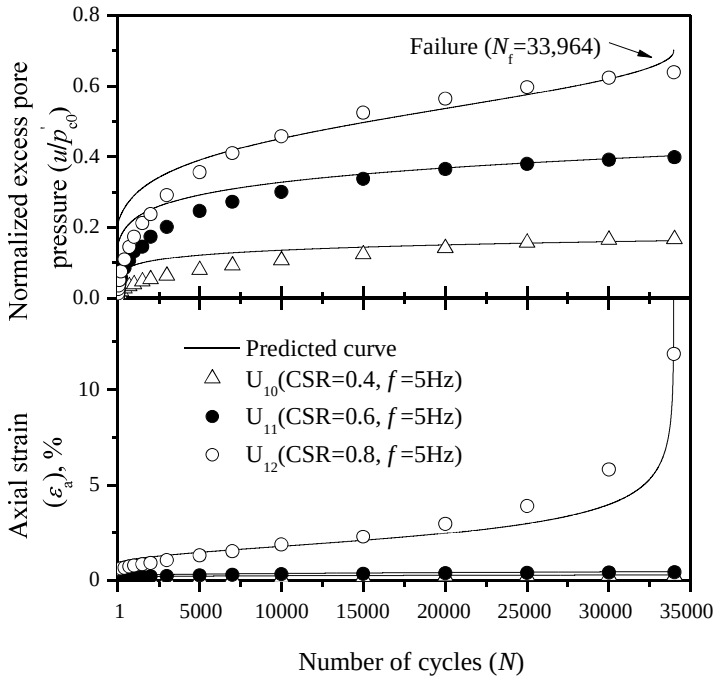


(b)

**Fig. 4.** Predictions of excess pore pressures and axial strains: (a) $f = 0.1$ , (b) $f = 5$

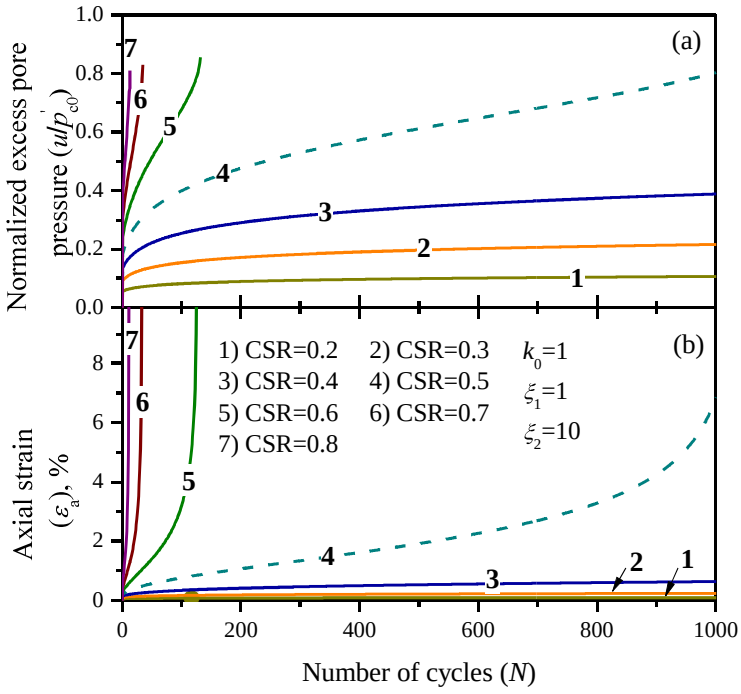


**Fig. 5.** Predictions of the proposed model with different cyclic stress ratios ( $k_0 = 1,\ \xi_1 = 1, \xi_2 = 10$ )

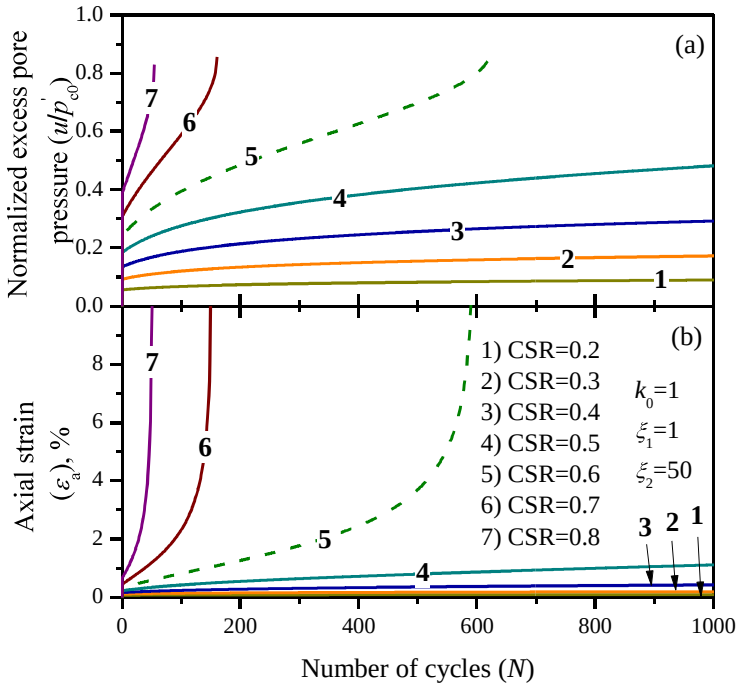


**Fig. 6.** Predictions of the proposed model with different cyclic stress ratios ( $k_0 = 1$, $\xi_1 = 1$, $\xi_2 = 50$ )

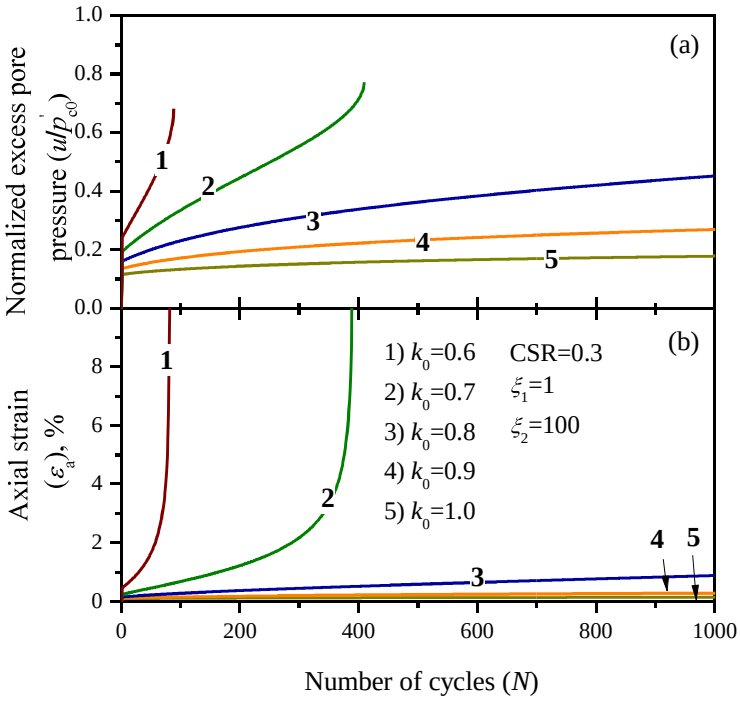


**Fig. 7**. Predictions of the proposed model with different anisotropic consolidation stress ratios ( $\mathrm{CSR} = 0.3$, $\xi_1 = 1$, $\xi_2 = 100$)

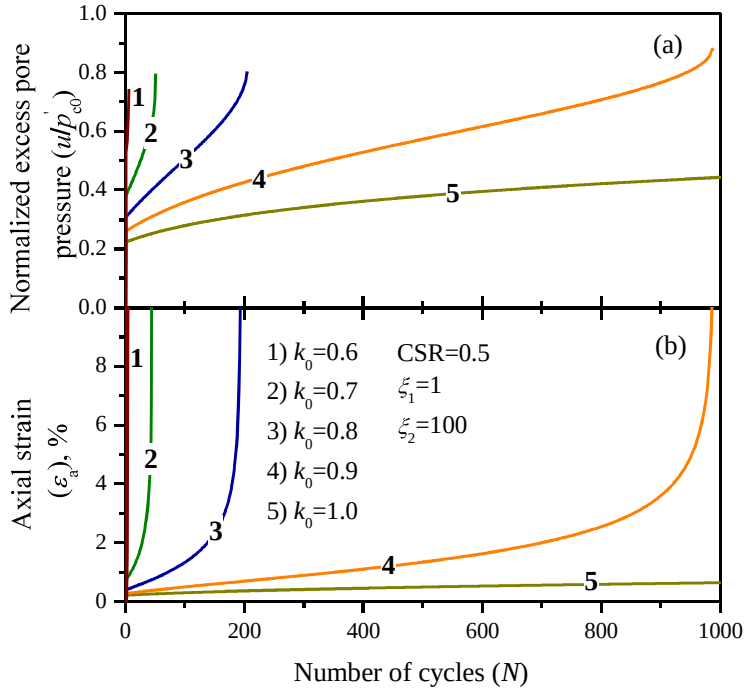


**Fig. 8.** Predictions of the proposed model with different anisotropic consolidation stress ratios ( CSR = 0.5 , $\xi_1$ = 1 , $\xi_2$ = 100)

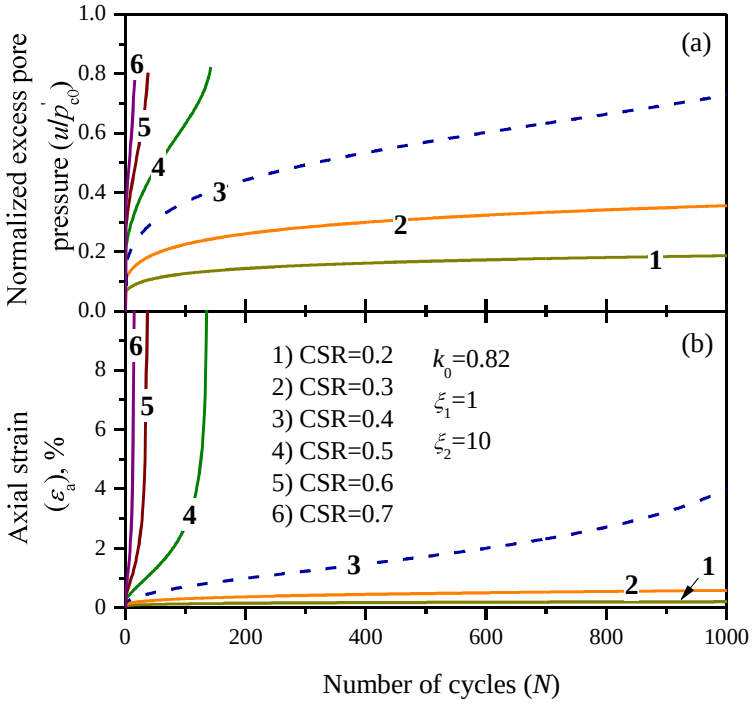


**Fig. 9.** Predictions of the proposed model with initial shear stress $k_0$ = 0.82

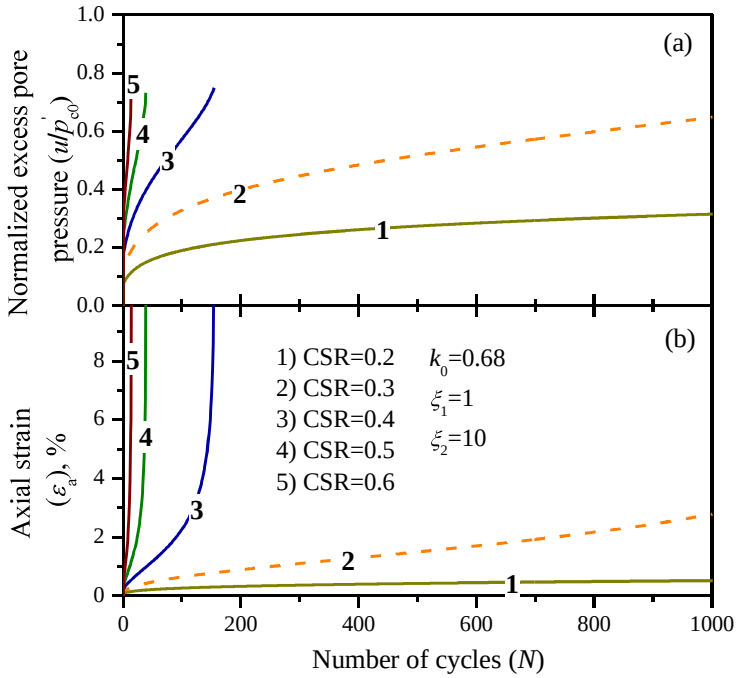


**Fig. 10.** Predictions of the proposed model with initial shear stress $k_0 = 0.68$

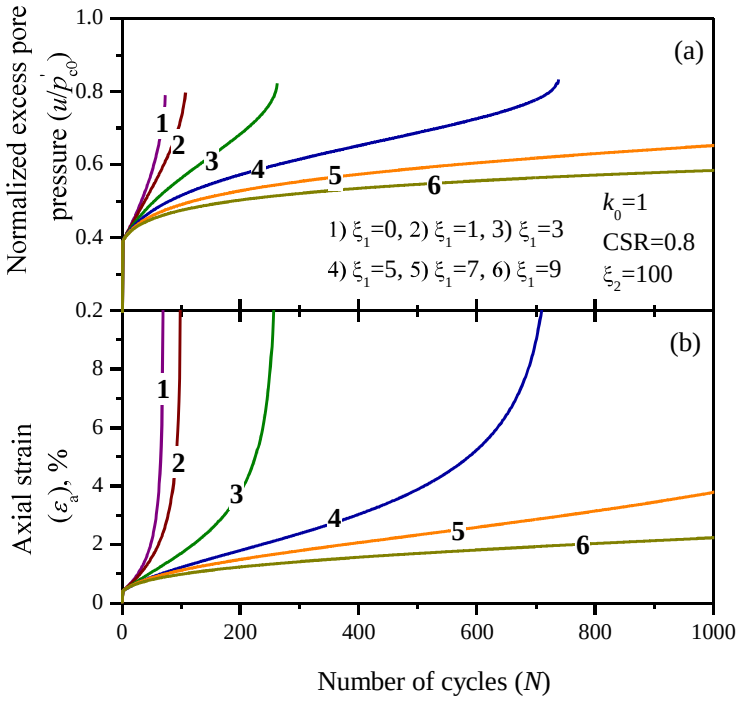


**Fig. 11.** Predictions of the proposed model with different values of $\xi_1$

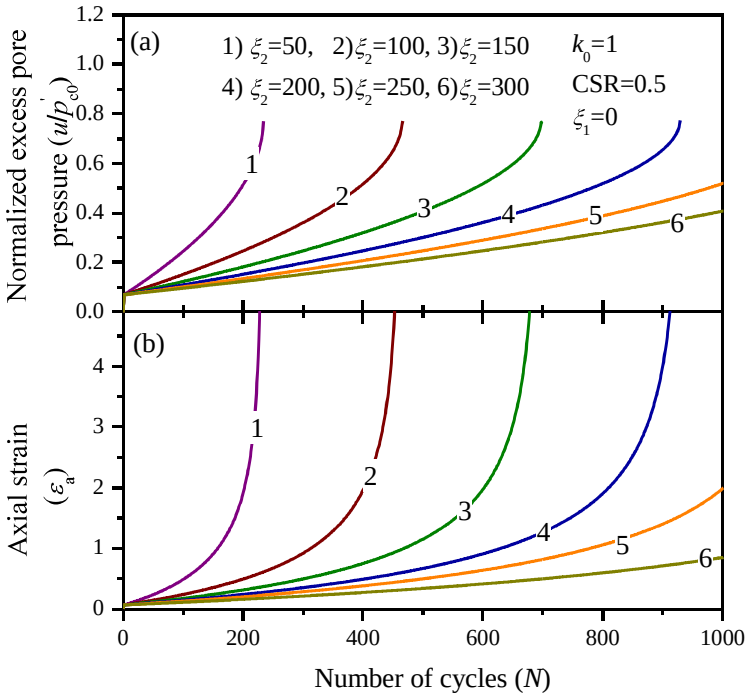


**Fig. 12.** Predictions of the proposed model with different values of $\xi_2$

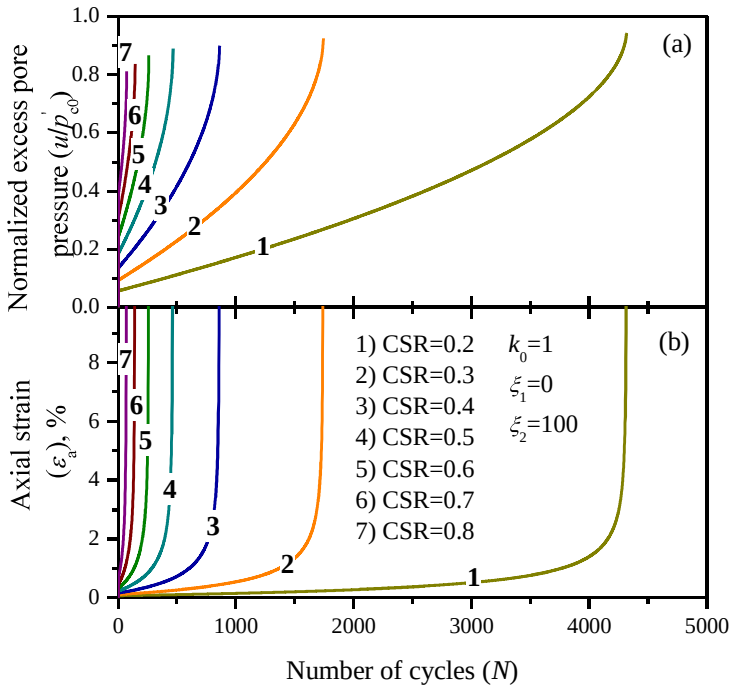


**Fig. 13.** Predictions of the proposed model with different cyclic stress ratios with $\xi_1 = 0$

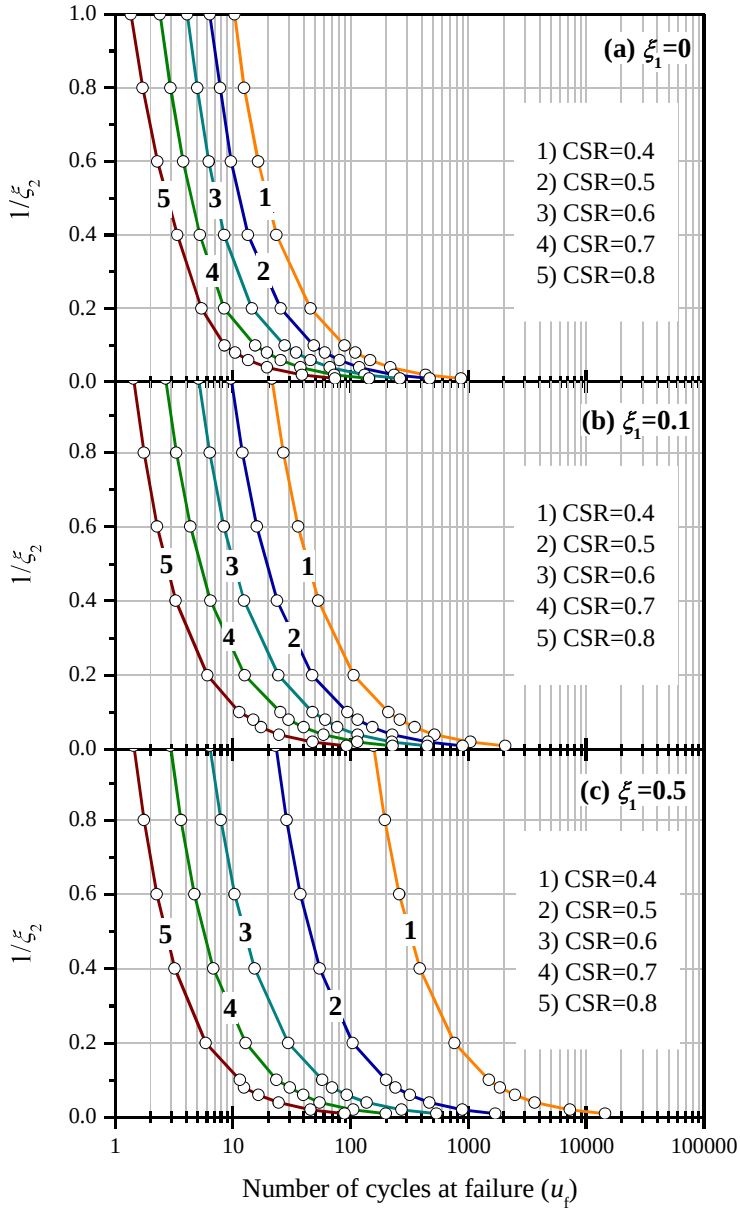


**Fig. 14.** The relationship between $1/\xi_2$ and number of cycles to failure ( $N_f$ )

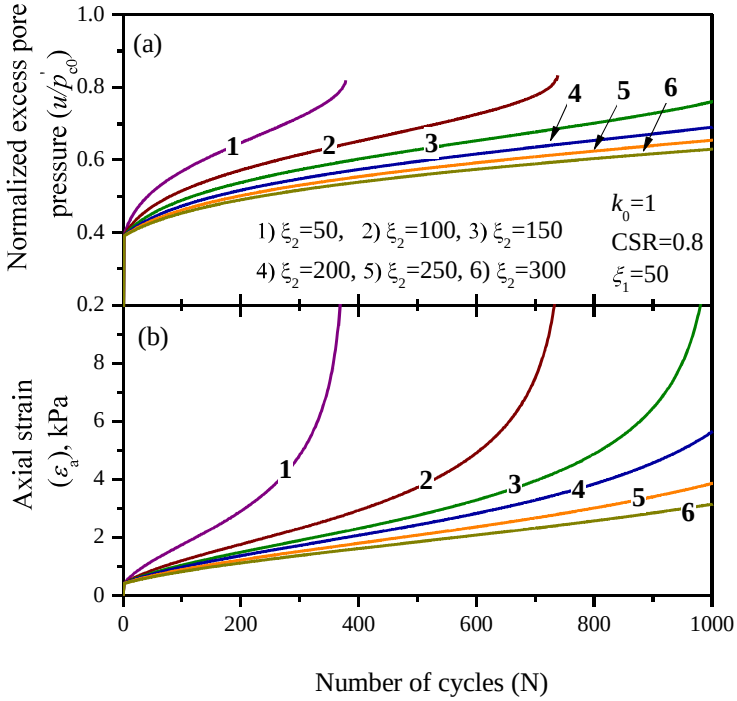


**Fig. 15.** Predictions of the proposed model with different values of $\xi_2$

**Table 1.** Summary of selected cyclic models for soft soils

| Source | Model Highlights | Shortcomings |
|---|---|---|
| Procter and Khaffaf (1984) | The relationship between cyclic stress level, loading frequency, and number of cycles at failure was modeled. | The development of excess pore pressure or axial strain during cyclic loading was not formulated. |
| Ansal and Erken (1989) | Regression expressions were developed to estimate the cyclic yield strength and excess pore pressure buildup based on the number of cycles and cyclic stress level. | The effect of the loading frequency was only experimentally investigated but not considered in the mathematical expressions. |
| Hyde et al. (1993) | Axial strain and normalized excess pore pressures were defined as a function of time-based power law. | A limitation of this model is that the predicted behavior of the soils is independent of the loading frequency. |
| Hyodo et al. (1994) | An exponential relationship for pore pressure against time was established and corresponding stability criteria were developed using the critical state line. | The effect of loading frequency is not taken into account. |
| Zhou and Gong (2001) | A mathematical model was presented to quantify the influence of cyclic stress level, loading frequency, and over-consolidation ratio. | A shortcoming of this model is that six parameters are introduced from regression expressions, but their method of determination was not elaborated. |

**Table 2.** Test conditions and results

| Specimen | Cyclic loading frequency ( $f$ ), Hz | Cyclic stress ratio ( CSR ) | Loading cycles ( $N$ ) | Failed or not |
|---|---|---|---|---|
| $U_{01}$ | 0.1 | 0.4 | 6,000 | No |
| $U_{02}$ | 0.1 | 0.6 | 6,000 | No |
| $U_{03}$ | 0.1 | 0.8 | 1,793 | Yes |
| $U_{04}$ | 1 | 0.4 | 34,466 | No |
| $U_{05}$ | 1 | 0.6 | 34,466 | No |
| $U_{06}$ | 1 | 0.8 | 10,419 | Yes |
| $U_{07}$ | 2 | 0.4 | 34,466 | No |
| $U_{08}$ | 2 | 0.6 | 34,466 | No |
| $U_{09}$ | 2 | 0.8 | 18,590 | Yes |
| $U_{10}$ | 5 | 0.4 | 33,000 | No |
| $U_{11}$ | 5 | 0.6 | 34,466 | No |
| $U_{12}$ | 5 | 0.8 | 33,964 | Yes |

**Table 3.** Parameters for soil properties and initial states

| Soil properties | | | | Initial states | | |
|---|---|---|---|---|---|---|
| $\lambda$ | $\kappa$ | $M$ | $p'_{c0}$ (kPa) | $p'_0$ (kPa) | $q_0$ (kPa) | $e_0$ |
| 0.18 | 0.03 | 1.68 | 30 | 30 | 16 | 1.32 |

**Table 4.** Parameters for cyclic loading

| Cyclic loading conditions | | | |
|---|---|---|---|
| $f$ (Hz) | Specimen | $\xi_1$ | $\xi_2$ |
| 0.1 | $U_{01}$, $U_{02}$, and $U_{03}$ | 2.8 | 50 |
| 1 | $U_{04}$, $U_{05}$, and $U_{06}$ | 2.7 | 280 |
| 2 | $U_{07}$, $U_{08}$, and $U_{09}$ | 2.7 | 400 |
| 5 | $U_{10}$, $U_{11}$, and $U_{12}$ | 2.8 | 550 |

**Table 5**. Parameters for undrained model analysis

| $\lambda$ | $\kappa$ | $M$ | $p'_{c0}$ (kPa) | $p'_0$ (kPa) | $e_0$ | $G$ |
|---|---|---|---|---|---|---|
| 0.25 | 0.05 | 1.2 | 30 | 30 | 0.6 | $200s_{u0}$ [a] |

[a] $s_{u0} = p'_{c0}\left(M/4\right)\left(2p'_0/p'_{c0}\right)^{\kappa/\lambda}$